

# WALL SHEAR STRESS DETERMINATION IN BOUNDARY LAYERS WITH UNKNOWN LAW OF THE WALL BY A MODIFIED PRESTON TUBE METHOD †

ICAS-82-6.4.2

C. HABERLAND and W. NITSCHKE

Institut für Luft- und Raumfahrt (ILR)  
Technical University of Berlin

## ABSTRACT

For determining local skin friction forces a measuring technique based on the Preston tube method is presented which allows the experimental determination of wall shear stress in boundary layers when these are influenced by additional parameters such as adverse pressure gradient, heat transfer, wall roughness and compressibility.

This method has been extended to a computational Preston tube method (CPM) in order to enable the application of this measuring technique even for arbitrary flow with unknown law of the wall. In this general method which does not require any calibration, the stagnation pressures of two Preston tubes with different diameters are used simultaneously for the computational determination of the resulting wall shear stress by means of iteration. The new method has been verified in the laminar-turbulent transition flow of a flat plate and in the entrance flow of a pipe.

Finally, a first idea is presented how the measuring technique could be applied in three dimensional boundary layer flows.

## 1. INTRODUCTION

Performance optimization of modern aircraft as well as ground vehicles requires an accurate theoretical or experimental drag prediction. Besides total drag measurements in a wind tunnel, it is desirable to determine directly the local skin friction for more sophisticated investigations: Applying advanced numerical calculation methods including viscous effects, it becomes necessary to compare the calculated wall shear stress distribution with the experimental one measured in a wind tunnel or in full scale flight tests. Hence, the applicability and limitations of numerical methods can be shown. On the other hand, the local shear stress has to be known for an experimental verification of the law of the wall used in calculation methods, since this shear stress - as a consequence of the similarity theory - is an implicit element of the boundary layer laws.

An often preferred method of measuring local skin friction in turbulent boundary layers represents the Preston tube method which, in contrast with other measuring techniques of experimental aerodynamics, allows a very simple determination of skin friction by measuring the stagnation pressure of a wall Pitot tube. However, prerequisite for this method in its original form is the validity of the universal law of the wall across the probe dia-

meter. For flows satisfying this prerequisite an universal calibration curve can be formulated correlating the Preston tube stagnation pressure and the local wall shear stress. This calibration curve is exactly valid only for classical boundary layer flows (turbulent flat plate and pipe flow) and can lead to significant measuring errors if the boundary is influenced by additional parameters, such as adverse pressure gradient, heat transfer, wall roughness and compressibility. This fundamental dependence on boundary layer parameters is a consequence of the measuring principle: The adjacent Preston tube stagnation pressure is proportional to the velocity at the effective wall distance of the probe and depends on the parameters which influence the velocity distribution of the boundary layer. Thus, the calibration curve is universal in such extent only, as the boundary layer law itself.

Therefore, a first objective of the present study has been to develop a more generally applicable measuring method allowing the reliable determination of wall shear stress in those flow types with additional boundary layer parameters. For this purpose, theoretical and experimental investigations have been performed which result in a set of calibration curves as well as an iteration method for measuring wall shear stress in non-classical boundary layer flows. Based on this analytical calibration curves, for a more practical application correction functions are derived leading to a simplified method of wall shear stress determination by means of iteration. In addition, correction functions have been derived considering simultaneously the influence of several boundary layer parameters, e.g. heat transfer and compressibility.

Although in contrast to the classical Preston tube method, which can be used without qualification only in flows which can be described by the universal turbulent wall law, the developed extended measuring technique offers a considerably wider range of application, it is still limited to boundary flows with known law of the wall, and as a consequence of the analytical treatment its reliability depends on the validity of each wall law. However, for practically interesting flow types the law of the wall is often not known. For this reason, the investigations concentrated on how to overcome these restrictions and in particular on the development of a new measuring technique by modifying the developed "extended" measuring method to a more computational one. In this Computational Preston tube Method (CPM) which does not require any calibration, the stagnation pressures of two Preston tubes with different diameters are used simultaneously for the computation of the resulting wall shear stress by means of iteration.

This "modified" Preston tube method is valid

† This research was supported by the German Science Foundation

for two-dimensional boundary layer flow. Thus, a measuring method applicable in three-dimensional flows becomes desirable. Therefore, a first approach for this extension is presented.

## 2. NOTATIONS

$A^+$	Van Driest's constant
$a$	speed of sound
$c_f = \tau_w / (\rho u_\infty^2)$	skin friction coefficient
$c_p$	specific heat
$D$	pipe diameter
$d$	Preston tube diameter
$d^+ = u_\tau d / \nu$	non-dimensional Preston tube diameter
$h$	sublayer fence height
$K$	displacement factor
$K_{1,2,\dots,i}$	iteration parameter of the boundary layer law
$k_s$	equivalent sand roughness
$k^+ = u_\tau k_s / \nu$	boundary layer roughness parameter
$L$	running length
$M_\tau = u_\tau / a_w$	friction Mach number
$p$	static pressure
$p^+ = [\nu / (\rho u_\tau^3)] \frac{dp}{dx}$	boundary layer pressure parameter
$Pr$	Prandtl number
$q^+ = qd^2 / (4\rho\nu^2)$	non-dimensional Preston tube stagnation pressure
$q$	Preston tube stagnation pressure
$\dot{q}$	heat transfer rate
$Re$	Reynolds number
$T$	temperature
$u$	mean flow velocity
$u^+ = u / u_\tau$	non-dimensional mean velocity
$u_\tau = \sqrt{\tau_w / \rho}$	shear stress velocity
$w$	cross flow velocity
$w^+$	non-dimensional cross flow velocity
$x$	mean flow direction co-ordinate
$y$	distance from wall
$y^+ = u_\tau y / \nu$	non-dimensional distance from wall
$z$	cross flow direction co-ordinate
$\alpha_o$	cross flow angle
$\beta_q = \dot{q}_w / (\rho c_p T) u_\tau$	heat transfer parameter
$\delta$	boundary layer thickness
$\delta^+$	non-dimensional boundary layer thickness
$\kappa$	Kármán constant
$\lambda = 8\tau_w / (\rho u_m^2)$	friction factor
$\rho$	density

$\tau$	shear stress
$\tau^+ = \tau_w d^2 / (4\rho\nu^2)$	non-dimensional wall shear stress
$\nu$	kinematic viscosity

## Subscripts

$D$	diameter
$e$	edge of the boundary layer
$f$	fluid
$l$	left side
$m$	mean value
$r$	right side
$t$	turbulent
$w$	wall conditions
$x$	mean direction
$z$	cross direction
$\infty$	free stream conditions
$0$	reference condition

## 3. STATE OF ART

The measuring technique of determining the local wall shear stress by a stagnation pressure measurement with a wall Pitot tube, developed by PRESTON (1) has been corroborated principally by numerous researchers, e.g. PATEL (2), NPL (3), RECHENBERG (4), BERTELROD (5). The identical results of these mainly experimental investigations are Preston tube calibration curves either of the form

$$q^+ = F(\tau^+) \quad (1)$$

$$q^+ = \frac{q d^2}{4 \rho \nu^2}; \quad \tau^+ = \frac{\tau_w d^2}{4 \rho \nu^2} \quad (2)$$

or of the type

$$\frac{q}{\tau_w} = F(\tau^+), \quad (3)$$

which both provide an unique correlation of the measured stagnation pressure with the local wall shear stress. In (6) it has been demonstrated that these calibration curve can also be calculated when integrating the similarity law of the velocity boundary layer

$$u^+ = \int_0^{y^+} f(y^+) dy^+; \quad u^+ = \frac{u}{u_\tau}, \quad y^+ = \frac{u_\tau y}{\nu} \quad (4)$$

across the probe diameter. Thus, using the resulting analytical approach for the Preston tube calibration curve

$$q^+ = \frac{1}{2} \tau^+ \left\{ \int_0^{y^+} f(y^+) dy^+ \right\}^2 \quad (5)$$

in conjunction with the "universal" law of the wall for velocity boundary layers according to VAN DRIEST (7), the analytical calibration curve for developed turbulent pipe and flat plate flow can be computed by means of numerical integration of the boundary layer law:

$$q^+ = \frac{1}{2} \tau^+ \left\{ \int_0^{y^+} \frac{2 dy^+}{1 + [4(\kappa y^+)^2 (1 - e^{-y^+/A^+})^2]^{0.5}} \right\}^2$$

$$\kappa = 0.4 ; A^+ = 26 . \quad (6)$$

This equation can be brought in a form comparable to that of equ. (2) and (3) when the coordination between the non-dimensional wall distance  $y^+$  and the shear stress variable  $\tau^+$  is introduced in equ. (6)

$$y^+ = K \sqrt{\tau^+} . \quad (7)$$

Therein K represents a displacement factor which, with respect to the Preston tube diameter  $d$ , establishes the effective wall distance

$$y_{\text{eff}} = \frac{d}{2} K , \quad (8)$$

for which the velocity determined from the measured stagnation pressure corresponds to the actual velocity distribution in the boundary layer.

Figure 1 shows a comparison between the calculated calibration curve and the experimental results obtained by PRESTON, NPL and PATEL. It is obvious that the computation well describes the experimental calibration curves, particularly the frequently used curve by PATEL.

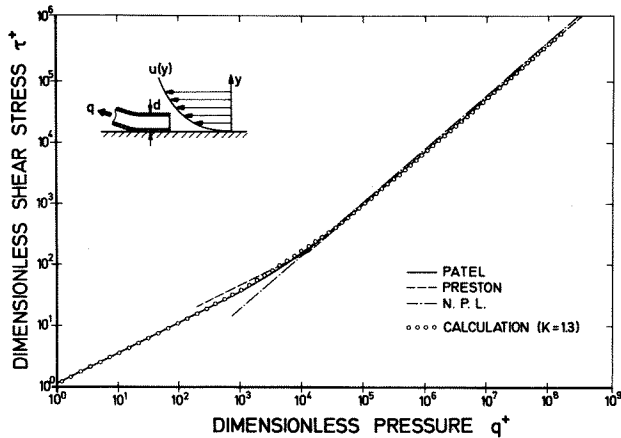


Figure 1. Wall shear stress calibration curve for Preston tubes. Non-dimensional wall shear stress dependent on non-dimensional stagnation pressure.

In a first approach figure 1 has been calculated with a displacement factor  $K = 1.3$  due to investigations by MC MILLAN (8) for small Preston tube diameters and ratios  $d_i/d_o \geq 0.6$ , figure 2a.

However, when comparing the wall shear stress calculated with  $K = 1.3$  with the stress resulting from the classical calibration curve, figure 3, yields a maximum error of 8 %, figure 2b. Applying instead of  $K = 1.3$  the relation  $K = f(d^+)$  recommended by MCMILLAN (8), figure 2a, the calculation leads to an unessential improvement, figure 2b. But, using the empirically determined K-distribution of figure 2a, a significant increase of the accuracy can be realized. Hence, the difference between the calculated and the reference calibration curve can be scaled down underneath 1 %.

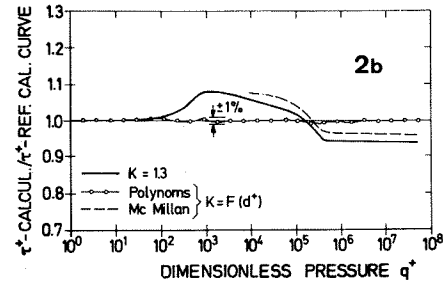
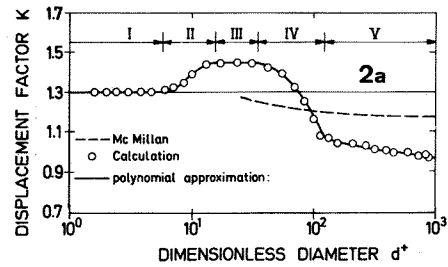


Figure 2. Influence of the displacement factor on the calculated Preston tube calibration curve.  
2a: Displacement factor dependent on dimensionless diameter  
2b: Normalized shear stress dependent on dimensionless pressure.

As the reference calibration curve ("classical" calibration curve) for the stagnation pressure ranges  $0 < \log q^+ < 2.9$  and  $5.6 < \log q^+ < 7.6$  the correlation obtained by PATEL (2) has been used:

$$0 < \log q^+ < 2.9$$

$$\log \tau^+ = 0.5 \log q^+ + 0.037 \quad (9a)$$

$$5.6 < \log q^+ < 7.6$$

$$\log q^+ = \log \tau^+ + 2 \log (1.95 \log \tau^+ + 4.1) \quad (9b)$$

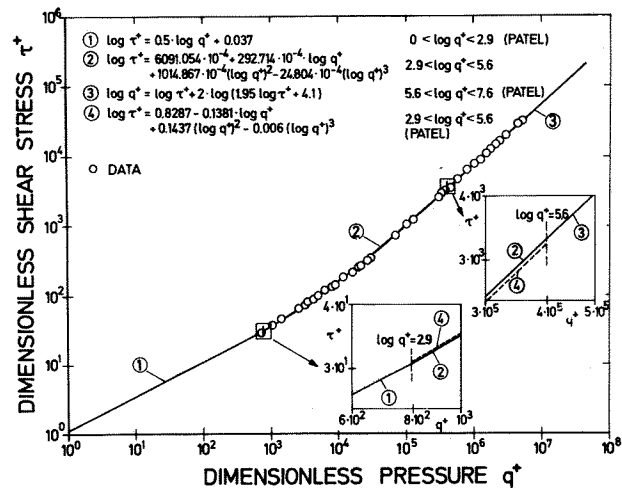


Figure 3. "Classical" Preston tube calibration curve. Non-dimensional wall shear stress dependent on the non-dimensional stagnation pressure.

For the midrange of the calibration curve an own, in contrast to the solution by PATEL improved polynomial equation has been developed:

$$2.9 < \log q^+ < 5.6$$

$$\log \tau^+ = 6091.054 \cdot 10^{-4} + 292.714 \cdot 10^{-4} \log q^+ + 1014.867 \cdot 10^{-4} (\log q^+)^2 - 24.804 \cdot 10^{-4} (\log q^+)^3 \quad (9c)$$

which guarantees a smoother adaption at the points of intersection of this 3-range calibration curve, figure 3.

#### 4. CALIBRATION CURVES FOR KNOWN LAW OF THE WALL

As a consequence of the direct coupling of boundary layer law and resulting Preston tube calibration curve the classical Preston tube method is applicable without any limitations for special flow types only, such as turbulent flat plate and pipe flow. To overcome these constraints, in (6) a more generally applicable wall shear stress measuring technique has been developed based on the analytical approach in equ. (5), rendering possible the reliable determination of Preston tube calibration curves from the boundary layer similarity laws even when additional parameters are introduced. It allows a calculation of sets of calibration curves dependent on the non-dimensional boundary layer parameters

$$p^+ = \frac{\nu}{\rho u_\tau^3} \cdot \frac{dp}{dx} \quad \text{pressure gradient} \quad (10)$$

$$\beta_q = \frac{\dot{q}_w}{(\rho c_p T)_w u_\tau} \quad \text{heat transfer} \quad (11)$$

$$k^+ = \frac{k_s u_\tau}{\nu} \quad \text{wall roughness} \quad (12)$$

and additionally to (6)

$$M_\tau = \frac{u_\tau}{a_w} \quad \text{friction Mach number} \quad (13)$$

as well as an iterative determination of the wall shear stress from measured Preston tube stagnation pressure and the parameters available in experiment:  $k_s$  (equivalent sand roughness),  $dp/dx$  (local pressure gradient),  $\dot{q}_w$  (local heat transfer rate) and  $a_w$  (speed of sound).

#### 4.1 Theoretical background

##### Calibration curves for additional parameters

The wall law in equ. (6) that applies to the classical flat plate and pipe flow must be replaced when additional boundary layer parameters have to be considered. For the parameters wall roughness, positive pressure gradient, heat transfer and compressibility the literature provides equations based on VAN DRIEST'S wall law:

##### Adverse pressure gradient

In many practical flows, such as diffuser or wing flow the variation of the static pressure with the running length can't be neglected. In particular, the pressure increase can lead to a reduced

skin friction at the wing and possibly to flow separation with vanishing skin friction.

Applying the wall law for boundary layer flow with positive pressure gradient of SZABLEWSKI (9), the set of Preston tube calibration curves dependent on the non-dimensional pressure parameter  $p^+$ , equ. (10), can be calculated from

$$q^+ = \frac{1}{2} \tau^+ \left\{ \int_0^{y^+} f(y^+, p^+) dy^+ \right\}^2 \quad (14)$$

$$f(y^+, p^+) = \frac{2(1+p^+y^+)}{1 + [1 + 4(\kappa y^+)^2 (1+p^+y^+) (1 - e^{-y^+ \sqrt{1+p^+y^+}/A^+})^2]^{0.5}}$$

$$\kappa = 0.4 ; A^+ = 26 \exp(-5.0 p^+) .$$

The used dependence of the VAN DRIEST damping constant on the pressure parameter is obtained from an experimental boundary layer investigation at an inclined flat plate (10).

##### Heat transfer

The basic theory of wall friction measurement developed by PRESTON, as well as the experimentally or analytically determined calibration curves are valid only for adiabatic flows with very small differences between wall and fluid temperature. But, in boundary layer flows with significant differences the influence of the temperature field on the flow field can't be neglected. Hence, the heat transfer rate has to be taken into account when determining wall law and calibration curve, and in the analytical approach, equ. (5), the adiabatic wall law has to be replaced by

$$u^+ = F(y_w^+, \beta_q)$$

in which the heat flux parameter  $\beta_q$  describes the influence of the heat transfer on the flow field. As shown by ROTTA (11) (12), the function  $F$  results from a simultaneous integration of the coupled differential equations for these two fields:

$$\frac{dT^+}{dy^+} = \frac{1}{\left(\frac{1}{Pr} - \frac{1}{Pr_t}\right) + \frac{dy^+}{du^+} \frac{1}{Pr_t}} \quad (15)$$

$$\frac{du^+}{dy^+} = \frac{2}{1 + [1 + 4(\kappa y^+)^2 (1 - e^{-y^+/A^+})^2]^{0.5}} \quad (16)$$

$$\kappa = 0.4 ; A^+ = 26 ; Pr = 0.72$$

$$Pr_t = 0.88 \{ [1 - \exp(-y^+/23.5)] / [1 - \exp(-y^+/29.5)] \}^2$$

This boundary layer law yields the calculation of the calibration curves dependent on the heat flux parameter

$$q^+ = \frac{1}{2} \tau^+ \left\{ \int_0^{y_w^+} f(y_w^+, \beta_q) dy_w^+ \right\}^2 \quad (17)$$

### Wall roughness

Since wall roughness leads to increased friction coefficients this influence has to be considered. The calibration curves for boundary layer flow at rough walls can be calculated from the analytical approach equ. (5) and the wall law formulated by ROTTA (13) via a displacement equation as a function of the non-dimensional roughness parameter  $k^+$

$$q^+ = \frac{1}{2} \tau^+ \left\{ \int_0^{y^+} f(y^+, k^+) dy^+ \right\}^2 \quad (18)$$

$$f(y^+, k^+) =$$

$$\frac{2}{1 + [1 + 4\kappa^2 (y^+ + \Delta y^+)^2 (1 - e^{-(y^+ + \Delta y^+)/A^+})^2]^{0.5}}$$

$$\Delta y^+ = 0.9 [k^{+0.5} - k^+ \exp(-k^+/6)] \text{ acc. to CEBECI (14)}$$

$$A^+ = 26 \quad \kappa = 0.4$$

### Compressibility

To extend the Preston tube method to compressible flow one has to replace the wall law of the incompressible turbulent flow by the equation

$$u^+ = F(y_w^+, M_\tau, \beta_q)$$

in which the influence of compressibility on the velocity boundary layer is indicated by the friction Mach number as well as by the heat flux parameter. Just as in non-adiabatic flow, for the calculation of the wall law the combined equations of energy and motion have to be solved simultaneously. Following ROTTA (11) this calculation can be carried out with equation (16) and the energy equation (15) extended with respect to the dissipative heat generated in the boundary layer.

$$\frac{dT}{dy} = \frac{\dot{q}_w - u\tau_w}{c_p \left[ \frac{\tau_w}{Pr_t} \frac{dy}{du} + \eta \left( \frac{1}{Pr} - \frac{1}{Pr_t} \right) \right]} \quad (19)$$

yielding, with equ. (5), for the adiabatic flow ( $\dot{q}_w = 0$ ) the set of calibration curves

$$q^+ = f(\tau^+, M_\tau) \quad (20)$$

and for non-adiabatic boundary layer flow ( $\dot{q}_w \neq 0$ )

$$q^+ = f(\tau^+, M_\tau, \beta_q) \quad (21)$$

### Correction functions

A more practical application can be obtained when relating the wall shear stress, calculated from the analytical Preston tube calibration curves, to those derived from the classical calibration curve. The resulting ratio, the correction function is

$$\tau_{p^+}^+ / \tau_{p^+=0}^+ = F(q^+, p^+) \text{ pressure gradient}$$

$$\tau_{\beta_q^+}^+ / \tau_{\beta_q=0}^+ = F(q^+, \beta_q) \text{ heat transfer}$$

$$\tau_{k^+}^+ / \tau_{k^+=0}^+ = F(q^+, k^+) \text{ wall roughness}$$

$$\tau_{M_\tau^+}^+ / \tau_{M_\tau=0}^+ = F(q^+, M_\tau) \text{ compressibility}$$

The calculated Preston tube calibration curves as well as the correction functions cannot be used directly for the experimental determination of wall shear stress, since the boundary layer parameters  $p^+$ ,  $\beta_q$ ,  $k^+$  and  $M_\tau$  used in the computation are themselves dependent on the wall shear stress via the shear stress velocity  $u_\tau$ . For this reason, an iteration method has been developed allowing to determine the skin friction from the Preston tube stagnation pressure and the parameters available in experiments: heat flux, equivalent sand roughness, local gradient and speed of sound at the wall. In contrast to the application of the calculated calibration curves the correction functions lead to a more simplified wall shear stress determination which does not need a computer, as shown in (10).

### 4.2 Experimental setup

To verify the analytical results, experiments with respect to pressure gradient and heat transfer have been carried out in the thermo wind tunnel of the Institute of Aeronautics and Astronautics (ILR).

This testing plant, drawn schematically in figure 4, has been planned according to the wind tunnel principle and is equipped with separate hot and cold air circuits which both are supplied with automatically working control units for air velocity and temperature in the test section, and can be run continuously. A more detailed description of the wind tunnel is given in (15).

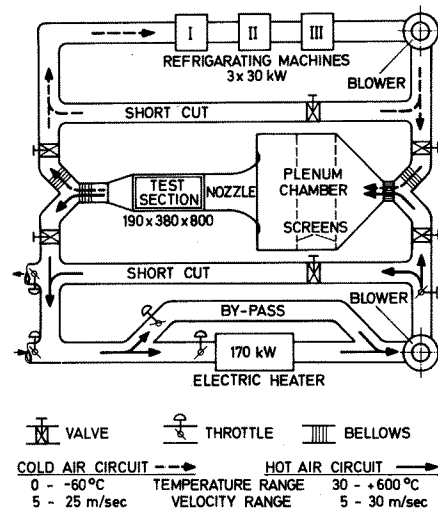


Figure 4. ILR thermo wind tunnel

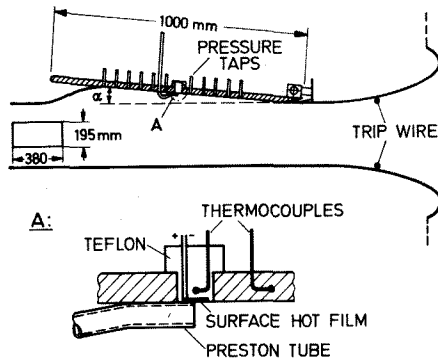


Figure 5. Test section and experimental arrangement of the thermo wind tunnel.

For the experimental investigations the thermo wind tunnel has been equipped with a test section wall that could be inclined to obtain a pressure gradient, figure 5, or with a heatable or coolable wall for studying heat transfer effects.

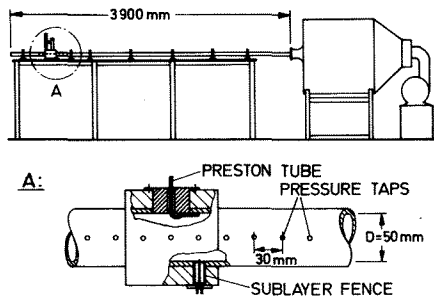


Figure 6. Test pipe and testing arrangement

The experiments for the Preston tube calibration curve influenced by wall roughness have been carried out in a fully developed pipe flow with two pipes of different rough walls. This special test pipe is shown in figure 6.

#### 4.3 Computational and experimental results

##### Sets of calibration curves

The sets of calibration curves dependent on the different influence parameters and calculated with equations (14) to (19). To check the quality of the "extended" Preston tube method, the results are compared with the experimental data measured in the thermo wind tunnel or the test pipe.

##### Pressure gradient

The experimental studies on the pressure gradient influence on the wall shear stress measurement have been carried out in a turbulent flow at a flat plate inclined in an angle of attack range against the section axis  $0 < \alpha < 20$  degree, figure 5, where also the arrangement of the measuring probes is shown. At the tip of the Preston tube the local wall shear stress has been determined by means of a sublayer fence (instead of the drawn hot film).

Figure 7 shows the significant influence of

the pressure gradient on the wall shear stress at high non-dimensional pressure and for  $p^+ = 0.0113$  and  $0.0223$  the good agreement between the calculated calibration curves and the experimental data.

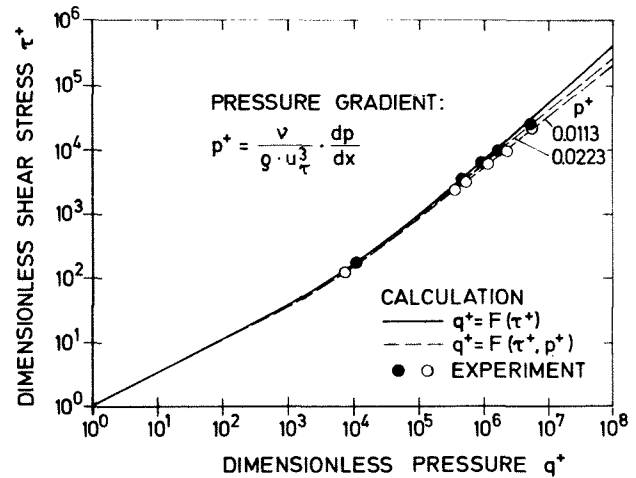


Figure 7. Wall shear stress calibration curve for Preston tubes in flows with adverse pressure.

For the experimental comparison of the calculated calibration curves, the non-dimensional Preston tube stagnation pressures  $q^+$  have been measured with variation of the probe diameter ( $1 \text{ mm} < d < 15 \text{ mm}$ ) at fixed experimental conditions ( $p^+ = \text{const.}$ ).

##### Heat transfer

Before calculating the calibration curves from the boundary layer law, equ. (15) and (16), attention should be paid to the dependence of the damping constant  $A^+$  on the heat flux parameter. For negative  $\beta_q$  ROTTA (12) gives the approximation

$$A^+ = 23.5 - 460 \beta_q,$$

which application for increasing positive  $\beta_q$  seems not to be useful. Since for positive  $\beta_q$  no investigations are known, the calculation has been carried out with  $A^+ = 26$ , the value for adiabatic flow.

For the experimental investigations at the heated or cooled wall of the test section, the air temperature has been varied in the range  $350^\circ > T_f > -60^\circ\text{C}$ , whereas the temperature of the test plate has been nearly constant ( $44^\circ > T_w > 19.5^\circ\text{C}$ ) which has been arranged by variation of the mass flow and temperature of the cooling or heating fluid (water). In this way resulting heat transfer rates  $-4.15 < \dot{q}_w < 12.9 \text{ [kW/m}^2\text{]}$  at flow velocities  $21.5 > u > 7 \text{ [m/sec]}$  could be obtained. The measuring and probe arrangement corresponded to the experiments with pressure gradient. In addition, with a thermoelement installed parallelly to the axis of the Preston tube the reference temperature for the density in the non-dimensional stagnation pressure equ. (2) has been determined. Corresponding to the calculations for the remaining properties in the calibration parameters  $q^+$  and  $\tau^+$  the measured local wall temperature has been used.

Figure 8 demonstrates the considerable influence of heat transfer on the calibration curve and also indicates the good agreement between the exper-

perimental data and the computed curves.

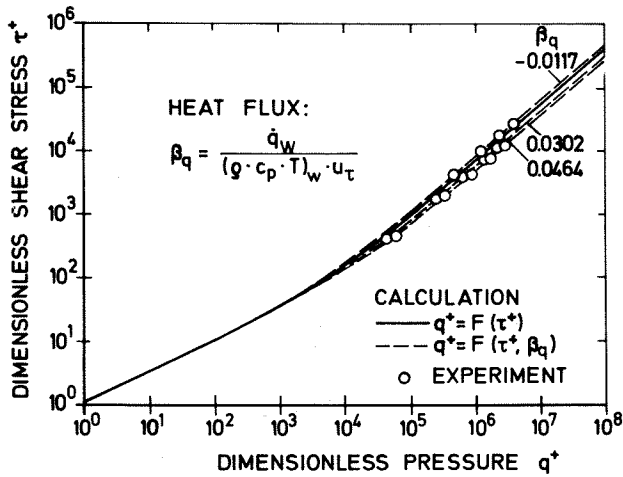


Figure 8. Wall shear stress calibration curve for Preston tubes in flows with heat transfer

Again, the measurements have been performed at fixed experimental conditions ( $\beta_q = \text{const.}$ ) and with Preston tube diameters  $1 < d < 5$  mm.

Wall roughness

The experimental investigation of the influence of the wall roughness have been carried out in the special test pipe, shown in fig.6, at a running length  $x/D = 70$ , at which due to the fully developed flow the local wall friction can be determined via the simple equilibrium equation between pressure and friction forces from the local pressure gradient

$$\tau_w = \frac{D}{4} \frac{dp}{dx}$$

For the experiments a smooth pipe with very good surface quality (drawn steel pipe) as well as a "rough" pipe with short wall waviness (extruded plexiglass) has been used. Again, the data have been measured at fixed test conditions ( $k^+ = \text{const.}$ )

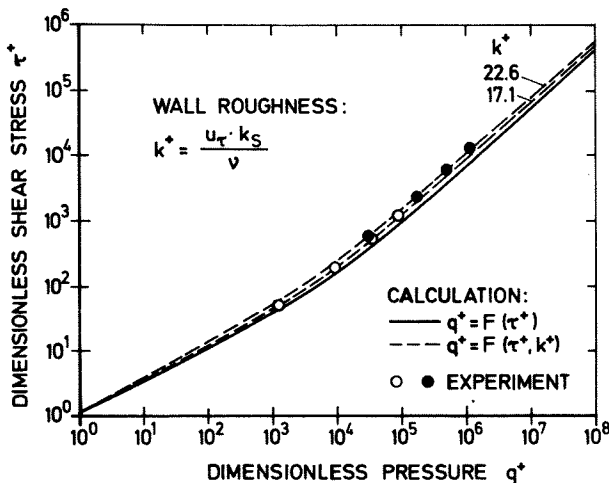


Figure 9. Wall shear stress calibration curves for Preston tubes at rough walls.

with variation of the stagnation pressure by applying different Preston tube diameters (0.5 mm <  $d < 2.3$  mm). The equivalent sand roughness which is decisive for the calibration curve calculation according equ. (18) has been determined from a comparison of the experimental data with the results at sand rough pipes obtained by NICURADSE, and ranges for the investigated Reynolds numbers between  $0.23 < k_s < 0.52$ .

Figure 9 shows the analytical calibration curve calculated by means of equ. (18) which compares very well with the measured one.

Compressibility

Since there exist numerous investigations in the literature concerning the influence of compressibility on the Preston tube method, e.g. by BERTELROD (16), BRADSHAW/UNSWORTH (17), ALLEN (18) no own experiments have been performed. However, these studies concentrate on the more simple case of a compressible flow without heat transfer at the wall. Thus, in the first instance for the purpose of comparison merely the calibration curve calculations according to equation (20) are considered.

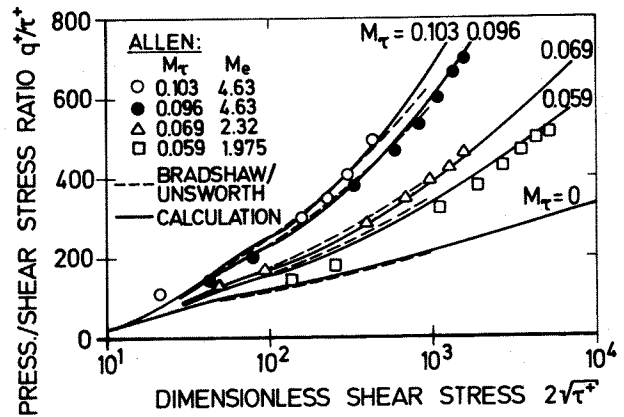


Figure 10. Wall shear stress calibration curves for Preston tubes in compressible flows

Figure 10 shows the calculated calibration curves compared to experimental results obtained by ALLEN (18), as quoted by BRADSHAW/UNSWORTH (17), as well as to an empirical calibration curve

$$\frac{q^+}{\tau^+} = 96 + 60 \log(d^+/50) + 23.7 [\log(d^+/50)]^2 + 10^4 M_\tau^2 (d^{+0.26} - 2) \tag{22}$$

for the incompressible flow range  $0 < M_\tau < 0.1$ , equally given in (17). In order to enable an accurate comparison of the experimental results as well as equation (22) with the computational results of the presented method, the appropriate boundary conditions according to the particular experiments of ALLEN have been used for the calculations: The density in  $q^+$  has been introduced at the local total temperature

$$T = T_w \left( 1 + \frac{\kappa-1}{2} M^2 \right), \quad \kappa = 1.4,$$

the remaining properties in  $q^+$  and  $\tau^+$  at wall temperature. In addition, the calculated incompressible Preston tube stagnation pressure has been converted to the measured compressible one by

$$q_{\text{compr.}} = \frac{2}{\kappa M^2} \left[ \left( 1 + \frac{\kappa-1}{2} M^2 \right)^{\frac{\kappa}{\kappa-1}} - 1 \right] q_{\text{inc.}}$$

As figure 10 demonstrates, the calculated calibration curves compare very well with the experimental results of ALLEN and the BRADSHAW/UNSWORTH formula.

The comparison of these calculated curves with equation (22) and the empirical calibration curve developed by BERTELROD

$$\frac{q^+}{\tau^+} = 38.85 \log(q^+ 4) - 107.3 + 10^4 M_\tau^2 (d^+)^{0.3} - 2.38, \quad (23)$$

but here changed to the more conventional plotting  $q^+ = f(\tau^+, M_\tau)$ , shows figure 11.

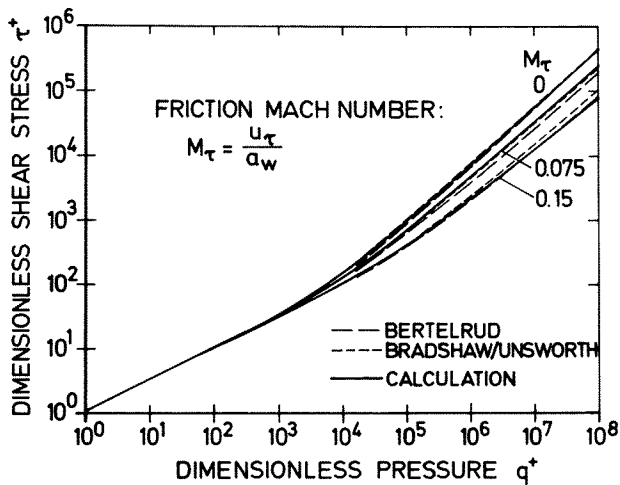


Figure 11. Wall shear stress calibration curves for Preston tubes in compressible flows.

Also this graph makes evident that the analytical calibration curves describe very satisfactory the influence of compressibility on the Preston tube calibration curve.

#### Correction functions

For a more practical application correction functions have been defined which relate the wall shear stresses calculated including additional boundary layer parameters to those derived from the classical calibration curve. These wall shear stress ratios are compared with the experimental data in the following figures. Naturally, in order to obtain the experimental correction function, the test conditions don't have been changed in comparison to those described in chapter "Sets of calibration curves".

#### Pressure gradient

In order to get the experimental data comparable with the analytical correction functions, the actual non-dimensional wall shear stress  $\tau_{p=0}^+$ ,

measured with a sublayer fence has been normalized with the wall shear stress  $\tau_{p=0}^+$  from the classical Preston tube calibration curve for the particularly measured stagnation pressures.

Figure 12 shows that the experimental data compare well with computational correction functions, verifying the reliability of the presented method.

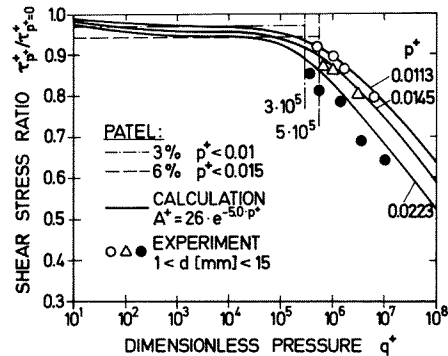


Figure 12. Preston tube correction functions for flows with an adverse pressure gradient.

In general, it can be stated that the calculated shear stress ratios for small non-dimensional Preston tube stagnation pressure parameters are near 1, corroborating PATEL'S estimation (2) of maximum errors of 3 % or rather 6 %. However, with increasing stagnation pressure and pressure parameter the influence of an adverse pressure gradient on the shear stress ratio increases and the error in measurement exceeds the limit of error stated by PATEL.

#### Heat transfer

In figure 13 some calculated correction functions are compared to the experimentally determined shear stress ratios:

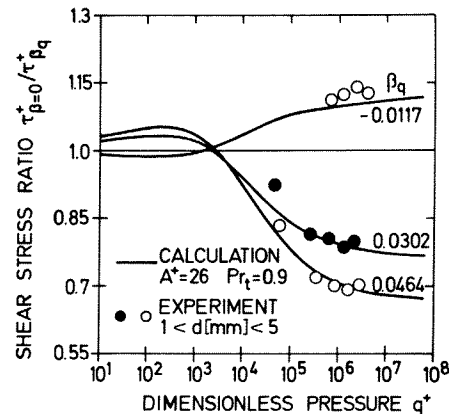


Figure 13. Preston tube correction functions for flows with heat transfer.

The figure shows that the calculation describes the experimental results satisfactory. The small deviations seem to be caused by the neglected dependence of the VAN DRIEST damping constant on the heat flux parameter  $\beta_q$ .

#### Wall roughness

Figure 14 clearly shows the strong influence of wall roughness on the normalized wall shear



stress. In the experimental correction ratio the actual wall shear stress has been determined from the pressure drop of the test pipe and normalized with the shear stress of the classical calibration curve corresponding with the particular Preston tube stagnation pressure.

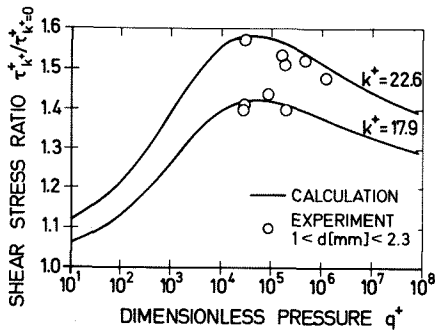


Figure 14. Preston tube correction functions for flows at rough walls.

As shown in the figure, the comparison yields a satisfactory agreement between calculated and measured correction functions.

#### Compressibility

The strong effect of compressibility, reducing the wall shear stress considerable compared to the classical calibration curve, clearly indicates figure 15. Since own measuring data don't have been available no experimental verification has been realized.

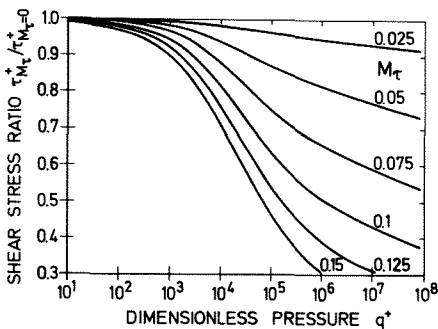


Figure 15. Preston tube correction functions for compressible flows.

Summarizing, the computed correction functions as well as the experimental results clearly show that the additional boundary layer parameters greatly influence the Preston tube calibration curve. Hence follows, that the determination of the wall shear stress without taking into account these parameters can lead to considerable measuring errors.

#### Simultaneous consideration of several boundary layer parameters

In realistic boundary layer flows, simultaneously several influence parameters have to be taken into account. In principle, the applied calculation technique allows the computation of calibration curves for different combinations of influence parameters.

For instance, in figure 16 the correction

functions for compressible flow with heat transfer are plotted which are calculated by means of the boundary layer law of ROTTA (11), equ. (16) and (19). It becomes obvious, that with increasing friction Mach number the shear stress ratio for a given heat flux parameter reduces considerably, indicating the great measuring errors not taking into account both parameters influencing the non-adiabatic incompressible boundary layer flow.

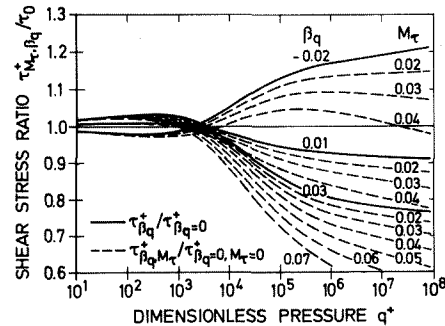


Figure 16. Preston tube correction functions for compressible flow with heat transfer.

For other combinations, such as compressibility and pressure gradient, heat transfer and wall roughness the correction functions can be calculated formally by means of superposition of the particular boundary layer laws.

In figure 17 simultaneously four influence parameter combinations are investigated: One finds the reducing influence of compressibility at constant wall roughness or constant pressure gradient, the increasing effect of wall roughness at constant heat transfer and the reduction of the wall shear stress with increasing pressure parameter at constant  $\beta_q$ .

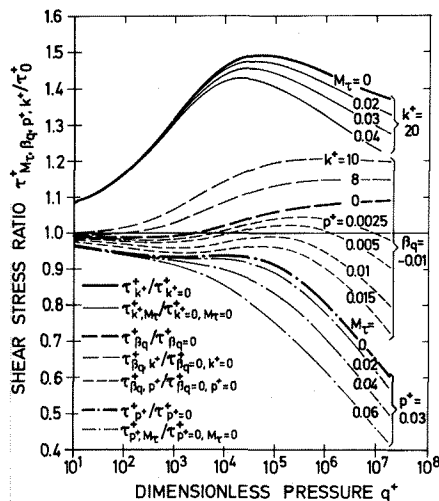


Figure 17. Preston tube correction functions considering combinations of heat flux -, wall roughness -, pressure gradient parameter and friction Mach number

Since the applicability of superimposed boundary layer laws is not known for certain, the above

graph should be regarded rather as a trend information than an exact solution of the particular flow problem.

## 5. PRESTON TUBE METHOD FOR UNKNOWN LAW OF THE WALL

As illustrated in the precedent chapter, also the application of the presented Preston tube method considering additional boundary layer parameters is limited since as a matter of principle a physically founded law of the wall is needed when determining the calibration curve or rather the wall shear stress. However, for numerous realistic flows the law of the wall has to be taken for unknown. Thus, the Preston tube method has to be modified for an application in such flows.

### 5.1 Theoretical background

The calculation of the particularly valid Preston tube calibration curves can't be performed with the boundary layer similarity laws only, but also from measured boundary layer velocity profiles. For this purpose, the particular non-dimensional velocities and distances from the wall are considered as discrete solutions of the analytical boundary layer approach in equ. (5) and the calibration curve calculation takes place by a point-by-point evaluation.

This is illustrated by the figures 18 and 19 which show investigations in the entrance region of a pipe flow:

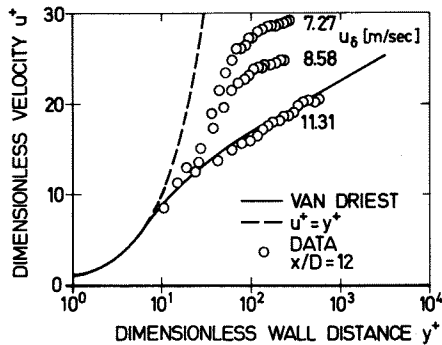


Figure 18. Non-dimensional boundary layer profiles in the entrance region of a pipe.

From the non-dimensional boundary layer profiles measured at a relative running length  $x/D = 12$ , figure 18, the resulting Preston tube calibration curves have been calculated point by point. Then, these computational results have been verified experimentally applying Preston tubes with different diameters at constant test conditions, figure 19. Herewith, the local wall friction has been measured with a sublayer fence calibrated at  $x/D = 70$ . Corresponding to the boundary layer flow with known law of the wall, the experimental results clearly confirm the correlation between the particular boundary layer profile and the Preston tube calibration curve. Thus, the intended modification of the Preston tube method for an application in flows with unknown wall law can base on the general possibility of calculating the calibration curve at single points. In addition, a further important prerequisite can be used: Applying measu-

ring probes with different diameters the particularly valid calibration curves supply identical wall shear stresses.

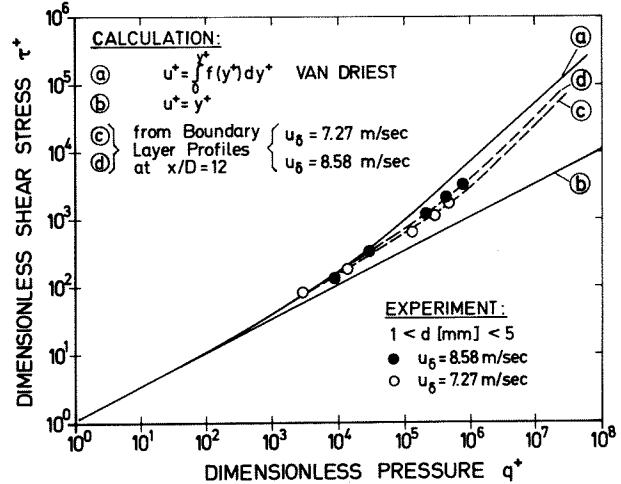


Figure 19. Preston tube calibration curves calculated from measured boundary layer profiles, compared to experimental results.

### 5.2 Computational Preston tube method

The developed computational Preston tube method is based on a wall law of the mathematical form

$$u^+ = \int_0^{y^+} \frac{2(1+K_3 y^+)}{0.5 \sqrt{1 + [4K_1^2 y^{+2} + (1+K_3 y^+)(1 - e^{-y^+ \sqrt{1+K_3 y^+}} / K_2)]^2}} dy^+ \quad (24)$$

which, in contrast to van Driest's law of the wall by means of the free parameters  $K_1$ ,  $K_2$  and  $K_3$  allows altered mixing lengths, changed damping constants in the analytical approach for the mixing length as well as a variation of the shear stress across the boundary layer as a function of the wall distance. The last parameter corresponds to the wall law with an adverse pressure gradient, equ. (14), where  $K_3 = p^+$ .

Figure 20 shows a parametric representation which illustrate the application range of this wall law. For  $K_1 = 0.4$ ,  $K_2 = 26$  and  $K_3 = 0$  this wall law becomes identical to van Driest's law which leads to the classical Preston tube calibration curve, equ. (6). Hence, this wall law represents the mathematical basis for the new Preston tube method which necessarily has to be a computer aided one: Starting-point is the calculated classical calibration curve ( $K_1 = 0.4$ ,  $K_2 = 26$ ,  $K_3 = 0$ ) which is applied to two measured Preston tube stagnation pressures obtained from two measuring probes with different diameter. In case that no coinciding wall shear stresses  $\tau_{W,1} = \tau_{W,2}$  result from both measured data, the controlling parameters  $K_i$  will be varied in such a way, that the calibration curve computed from the wall law yields identical shear stresses for both probes.

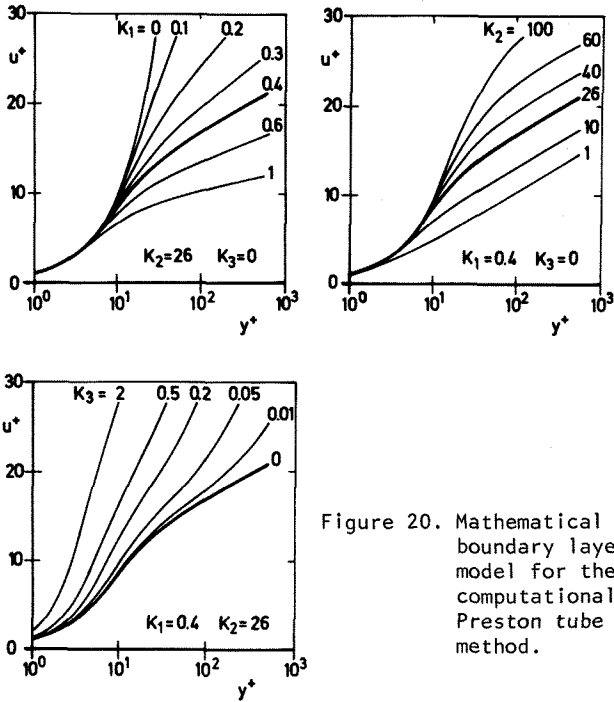


Figure 20. Mathematical boundary layer model for the computational Preston tube method.

The iterative procedure is summarized schematically in the syntax diagram of figure 21.

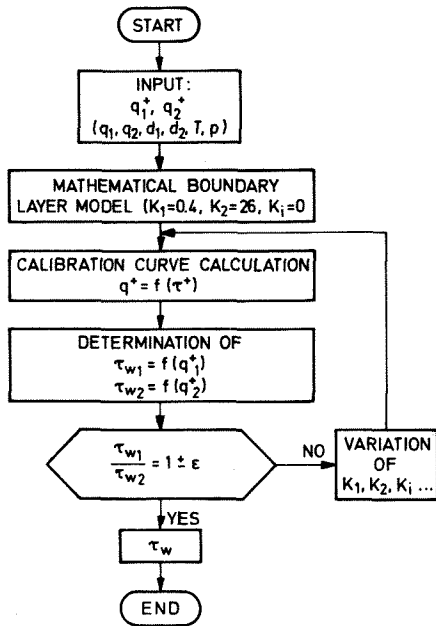


Figure 21. Syntax diagram for the computational Preston tube method.

More details of the method are shown in the figures 22 and 23. In figure 22, for the laminar-turbulent transition flow of a flat plate the boundary layer iteration is demonstrated for that controlling parameter  $K_1$  ( $K_1 = 0.15$ ), which satisfies both Preston tube measuring values which here are represented by the velocities calculated from the Preston tube stagnation pressures corresponding to

the two effective wall distances. Therefore, this parameter can be used for the calibration curve calculation.

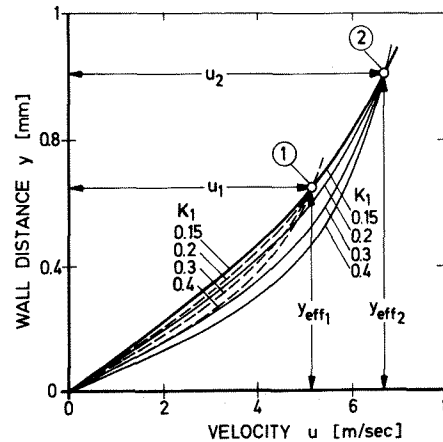


Figure 22. Boundary layer iteration for computational Preston tube method.

Again for the example of a  $K_1$ -variation, figure 23 explains the procedure of iteration which clearly shows the influence of the controlling parameter on the wall shear stresses  $\tau_{w,1}$  and  $\tau_{w,2}$  resulting from the particularly calculated calibration curves.

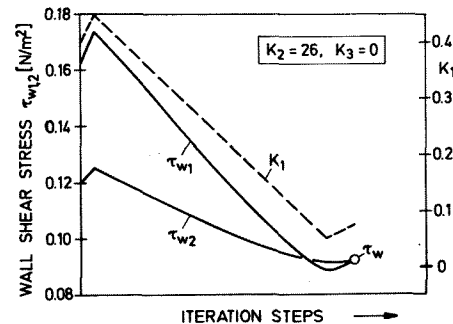


Figure 23. Wall shear stress iteration in the CPM-method.

## 5.1 Results

In order to check the quality of the developed CPM-method experimentally, wall shear stress measurements in the transition flow of a flat plate and a pipe entrance flow have been carried out. These test conditions have been selected since for these flow types large deviations of the boundary layer profiles from the classical van Driest wall law are to expect (see also figure 18) as well as no physical wall laws  $u^+ = f(y^+)$  are available.

### Transition flow

For the experimental investigation of the laminar-turbulent transition flow the test arrangement at the ILR-thermo wind tunnel has been used (figure 5). The transition flow has been generated by removing the trip wire in the contraction of test section.

Figure 24 shows for the turbulent flat plate flow which has been applied as calibration condition for the surface hot film used besides the Preston tubes, the good verification of the well known friction relation of SCHULZ-GRUNOW, independently of the diameter of the used Preston tube.

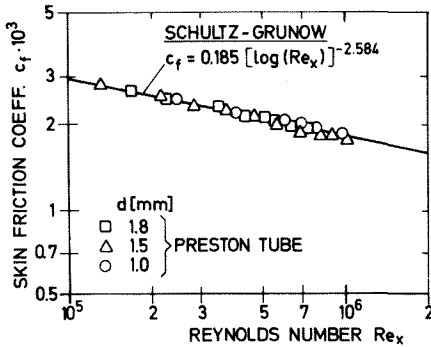


Figure 24. Measured skin friction coefficient of turbulent flat plate flow. Classical Preston tube data.

Contrary to that, applying the classical calibration curve for the laminar-turbulent transition flow and using Preston tubes with different diameters, the Preston tube results deviate considerably from each other, figure 25,

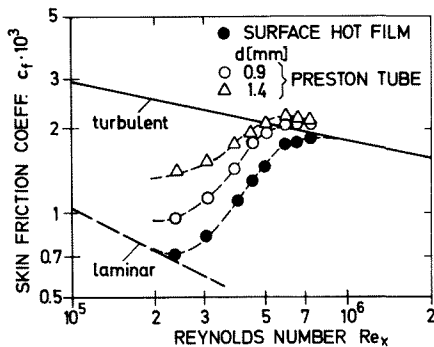


Figure 25. Measured skin friction coefficients of transition flow. Classical Preston tube and surface hot film data.

and are much higher than the surface hot film measuring data.

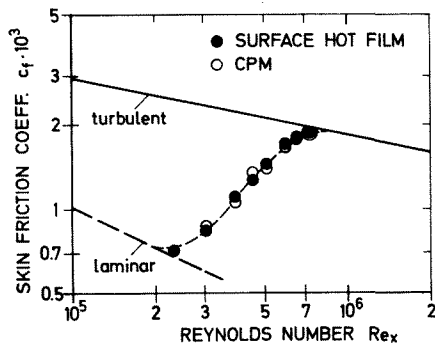


Figure 26. Measured skin friction coefficient of transition flow. CPM and hot film data.

On the other hand, figure 26 shows the results of the developed computational Preston tube method and indicates the good applicability of this measuring technique for this flow type. The two Preston tube stagnation pressures, needed for the CPM-method, have not been measured with two single probes of different diameters successively - as would be possible in principle - but simultaneously with a twin probe according to figure 27, which consists of two parallel tubes working without interference.

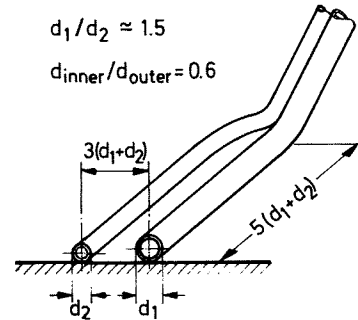


Figure 27. Twin probe used for the CPM-method.

#### Entrance flow of a pipe

For a further application of the developed CPM-method the wall friction in the entrance region of a pipe flow has been investigated. The experiments have been carried out in the test pipe according to figure 6, in which for developed flow ( $x/D = 70$ ) first of all the sublayer fence installed in the measuring cross section has been calibrated by means of the pressure drop.

Figure 28 shows the good agreement between the friction factors measured from the pressure drop as well as with the classical Preston tube method with different probe diameters, here compared to the theory according to BLASIUS.

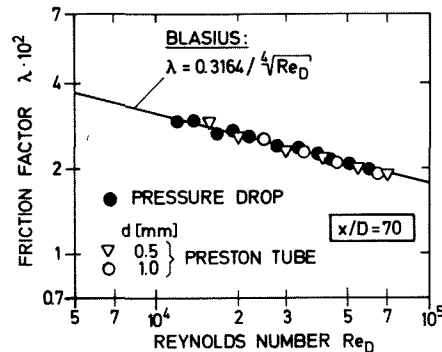


Figure 28. Measured friction factor in fully developed turbulent pipe flow. Pressure drop and Preston tube data.

For the same measuring arrangement but in its location shifted towards the entrance cross section ( $x/D = 5$ ) figure 29 shows the breakdown of the classical Preston tube method, indicated by the different measuring data obtained with the different Preston tubes, in comparison to the sublayer fence data.

In contrast, the CPM test data measured with a twin probe according to figure 27 correlate very well with measuring data of the sublayer fence, figure 30.

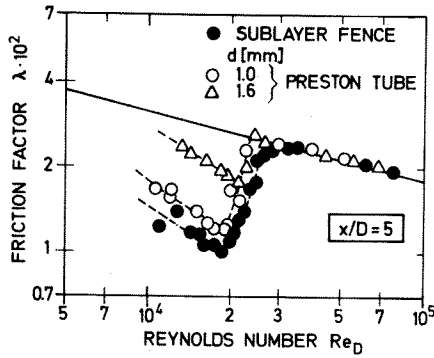


Figure 29. Measured friction factor in the entrance flow of a pipe. Classical Preston tube and sublayer fence data.

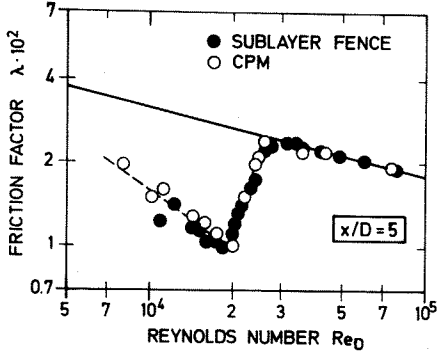


Figure 30. Measured friction factors in the entrance flow of a pipe. CPM and sublayer fence data.

The results clearly show that the developed computational Preston tube method is very well suited for an application in boundary layer flows with unknown law of the wall.

## 6. CALIBRATION CURVES FOR THREE-DIMENSIONAL FLOW

The intended extension of the Preston tube method to arbitrary boundary layer flows must consequently include the comprehension of three-dimensional flow types. Although in this paper the emphasis has been laid rather on the development of a modified, computational Preston tube method for unknown law of the wall than on a general treatment of all flow types, a first idea should be presented how such extension could happen.

### 6.1 Development of a three-dimensional measuring probe

It is known from the literature that applying the two-dimensional calibration curve for simple 3D-flows, wall shear stress measurements with tolerable measuring error become possible, as e.g. for a three-dimensional turbulent boundary layer behind a traverse hump in form of a 30° swept wing type model is shown in (19). However, the measurements confine themselves to the amount of wall friction, whereas as a consequence of the yaw characteristic of Pitot tubes the direction of the friction vector cannot be determined sufficiently accurate. Especially for boundary layer investigations this is a considerable drawback. If one demands amount as well as direction measured by a 3D-Preston tube technique, first of all a new probe type has to be developed measuring both compo-

nents. A suggestion for the design of such probe is shown in figure 31:

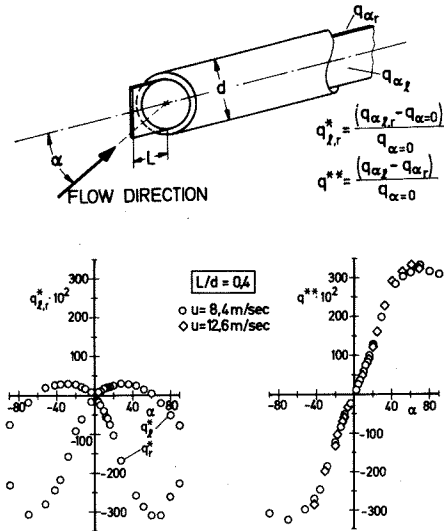


Figure 31. Two chamber probe for skin friction measurements in 3D-flows.

The conventional Preston tube has been separated into two measuring chambers by an edge which protrudes beyond the tube tip. The pressures of the two chambers can be measured separately. The basic idea of this measuring device is to describe the cross flow component of a three-dimensional flow by the differential pressure between the chambers which will be augmented by the edge, and the mean flow component by the mean value of both chamber pressures.

Because of its well-defined yaw characteristic this probe is applicable for yaw angles up to  $\pm 60$  degree, as demonstrated in the lower part of figure 31. From many tests an optimum ratio of length of the edge to probe diameter  $L/D = 0.4$  has been found.

### 6.2 First results

First experiments concerning the three-dimensional Preston tube method have been carried out in a 3D-boundary layer in front of a replacement body perpendicularly installed to the wall of the test section of the thermo wind tunnel. The oil flow picture in figure 32 indicates the three-dimensional character of the flow. The resulting skin friction has been measured with respect to amount and direction by means of a McCrosky surface hot film (20), which successfully has been applied in 3D-experiments by MEYER, KREPLIN (21) and BERTELUD (16). Prior to the particular experiments the hot film has been calibrated at the same place but without replacement body. At first, outside of the boundary layer and above the surface hot film the flow direction has been determined by means of rotatory two-chamber probes (not drawn in figure 32) and by balancing the chamber pressures. Then, after moving the measuring device towards the wall at this angular position the pressure difference  $q_1 - q_r$  as well as the mean value  $(q_1 + q_r)/2$  have been measured. The resulting measuring data yield the non-dimensional Preston tube stagnation pressures in the mean and cross flow direction according to the following equations

$$q_x^+ = \frac{(q_l + q_r) / 2 \cdot d^2}{4 \rho v^2} ; q_z^+ = \frac{(q_l - q_r) d^2}{4 \rho v^2} ,$$

which together with the non-dimensional shear stresses measured with surface hot films

$$\tau_x^+ = \frac{\tau_{wx} d^2}{4 \rho v^2} ; \tau_z^+ = \frac{\tau_{wz} d^2}{4 \rho v^2}$$

are shown in figure 33. The flow velocity has been  $u_\infty = 10$  m/sec, 4 different probe diameters have been used.

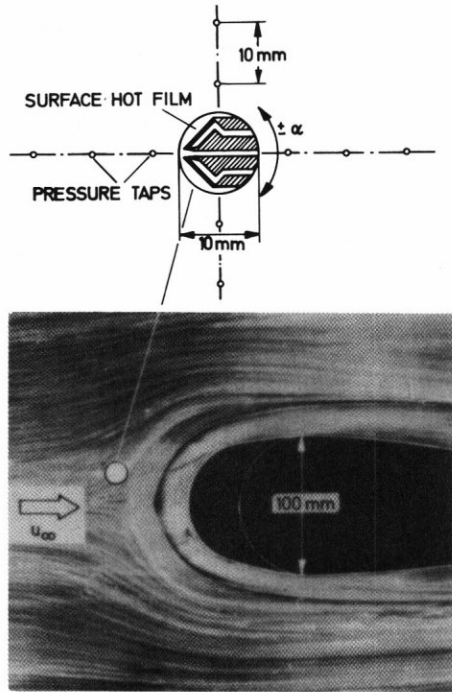


Figure 32. Experimental arrangement for three-dimensional flow investigation.

In this figure these experimental results also have been compared with first calculations of the calibration curve for known law of the wall. The calibration curve in mean flow direction has been calculated from the two-dimensional wall law for flows with pressure gradient, equ. (14), considering the 35 %-decreased stagnation pressure indication of the two-chamber probe compared to a conventional Pitot probe. The calibration curve of the cross flow component  $q_z^+ = F(\tau_z^+)$  has been calculated from the stagnation pressure relation of the transverse flow

$$q_z = \rho / 2 w^2 ,$$

the wall law for the cross component by MAGER (22)

$$w^+ = u^+ \tan \alpha_0 \left( 1 - \frac{y^+}{\delta^+} \right)$$

and the defining equation  $\tau_{wz} / \tau_{wx} = \tan \alpha_0 .$

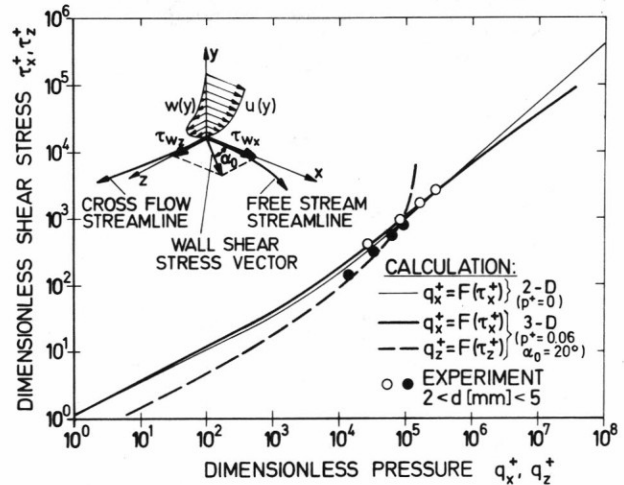


Figure 33. 3D-Preston tube calibration curves for mean and cross flow direction.

Additionally, the analytical stagnation pressure transverse to the flow direction has been corrected with the augmentation of the chamber pressure difference according to the characteristic in figure 31.

The satisfying agreement between experiment and calculation can be assigned as a first encouraging result with respect to an extension of the Preston tube method to three-dimensional flows. However, because of the complexity of this flow type very careful investigations will be necessary to get a deeper insight into the scope of applicability.

## 7. CONCLUDING REMARKS

Based on the concept of an extended Preston tube method for known law of the wall which allows the consideration of additional boundary layer parameters, a modified, computer aided measuring technique has been developed which appears to be capable to provide reasonable results for arbitrary 2D-flows with unknown law of the wall. However, real flow around bodies requires an extension of the theory to achieve a more general approach for an application to design optimization. Although a first idea for a 3D-method has been presented, future efforts for the following subjects will be necessary: The developed 2D-method for the unknown law of the wall should be verified in other flow types than those investigated in this paper. For this purpose, it has to be checked if the "mathematical" law of the wall used for the CPM-method has to be extended by introducing further iteration parameters with respect to the particular boundary layer flows. Furthermore, it should be investigated if this very general 2D-measuring technique can be applied for determining the mean shear stress in arbitrary 3D-flows.

Acknowledgements: The authors gratefully acknowledge the support from R. Thünker, N. Weiser and W. Pfingst in performing the extensive computations and wind tunnel testing.

## 8. REFERENCES

- (1) J.H. Preston: The determination of turbulent skin friction by means of Pitot tubes. *J. Roy. Aeron. Soc.* 58 (1954), pp. 109 - 121.
- (2) V.C. Patel: Calibration of the Preston tube and limitations on its use in pressure gradients. *J. Fluid Mech.* 23 (1965), pp. 185 - 203.
- (3) Staff of Aerodynamics Division, N.P.L.: On the measurement of local surface friction on a flat plate by means of Preston tubes. *ARC R. & M.* 3185 (1961).
- (4) I. Rechenberg: Messung der turbulenten Wandschubspannung. *Z. Flugwiss.* 11 (1963), pp. 429 - 438.
- (5) A. Bertelrud: Preston tube calibration accuracy. *AIAA Journ.* 14 (1976), pp. 98 - 100.
- (6) W. Nitsche: Wandschubspannungsmessung mit Prestonrohren in Grenzschichtströmungen mit zusätzlichen Einflußparametern. *Z. Flugwiss. Weltraumforsch.* 4 (1980) Heft 3, pp. 142 - 147  
Transl.: Measuring skin friction with Preston tubes in boundary layer flows with additional parameters. *Nat. Res. Council Canada, NRC/CNR TT-1989, Ottawa* (1981).
- (7) E.R. van Driest: On turbulent flow near a wall. *J. Aerospace Sci.* 23 (1956), pp. 1007 - 1036.
- (8) F.A. McMillan: Experiments on Pitot tubes in shear flow. *ARC R. & M.* 3028 (1956).
- (9) W. Szablewski: Turbulente Grenzschichten in Ablösenähe. *Z. angew. Math. Mech.* 49 (1969), pp. 215 - 225.
- (10) W. Nitsche, C. Haberland: Einfluß von Wandrauigkeit, Druckgradient und Wärmestrom auf die Wandreibungsmessung mit Prestonrohren. *Technische Universität Berlin, ILR-Bericht* 50 (1980).
- (11) J.C. Rotta: Über den Einfluß der Machschen Zahl und des Wärmeübergangs auf das Wandgesetz turbulenter Strömung. *Z. Flugwiss.* 7 (1959), pp. 264-274.
- (12) J.C. Rotta: Die turbulente Grenzschicht an einer stark geheizten ebenen Platte bei Unterschallströmung. *Wärme- und Stoffübertragung* 7 (1974), pp. 133 - 144.
- (13) J.C. Rotta: Turbulent boundary layers in incompressible flows. In: A. Ferri, D. Küchenmann, L.H.G. Sterne (Editors): *Progress in Aeronautical Sciences*, Vol. 2, pp. 1 - 219. Pergamon Press, Oxford/London/New York/Paris 1962.
- (14) T. Cebeci, K.C. Chang: Calculation of incompressible rough wall boundary layer flows. *AIAA-Journ.* Vol. 16, No. 7 (1978), pp. 730 - 735.
- (15) C. Haberland, W. Nitsche: Der Thermowindkanal des Instituts für Luft- und Raumfahrt der TU Berlin: Eine Mehrzweckanlage für aero-thermodynamische Grundlagenuntersuchungen. *DGLR-Paper* 81-030, *DGLR-Jahrestagung* (1981), Aachen.
- (16) A. Bertelrud: Instrumentation for measurement of flow properties on a swept wing in flight. *DGLR-Paper* 81-034, *DGLR-Jahrestagung* (1981), Aachen.
- (17) P. Bradshaw, K. Unsworth: A note on Preston tube calibrations in compressible flow. *I.C. Aero Report* 73 - 07 (1973).
- (18) J.M. Allen: Evaluation of compressible flow Preston tube calibration. *NASA TN D-7190* (1973).
- (19) K.S. Hebbar, W.L. Melnik: Wall region of a relating three-dimensional incompressible turbulent boundary layer. *Journ. Fluid Mech.* Vol. 85, part 1 (1978), pp. 33 - 56.
- (20) W.J. McCroskey, E.J. Durbin: Flow Angle and shear stress measurements using heated films and wires. *Journ. Basic Eng.* 94 (1972), pp. 46 - 52.
- (21) H.U. Meier, H.P. Kreplin: Experimental investigations of the boundary layer transition and separation on a body of revolution. *Z. Flugwiss. Weltraumforsch.* 4 (1980) Heft 2, pp. 65 - 71.
- (22) A. Mager: Generalisation of boundary layer momentum integral equations of three dimensional flows including those of rotating systems. *NACA Rep.* 1067 (1952).